Crustal structure from gravity signatures in the Iberian Peninsula

David Gómez-Ortiz[1,†], B.N.P. Agarwal[2], Rosa Tejero[3], and Javier Ruiz[3]
[1]*ESCET (Escuela Superior de Ciencias Experimentales y Tecnología), Área de Geología, Universidad Rey Juan Carlos, 28933 Móstoles, Spain*
[2]*Department of Applied Geophysics, Indian School of Mines, Dhanbad 826 004 (Jharkhand), India*
[3]*Departamento de Geodinámica, Universidad Complutense de Madrid, Jose Antonio Novais, 3, 28040 Madrid, Spain*

ABSTRACT

Through two-dimensional filtering and spectral analysis of gravity data, we infer the density structure of the Iberia Peninsula's lithosphere (western Europe). The gravity anomaly map of the Iberian Peninsula displays long-wavelength anomaly minima related to Alpine ranges. These anomalies are primarily linked to a greater crustal thickness. Low-pass filtering of the anomaly map using a cutoff wavelength of 150 km was adequate for effective separation of shallow and deep sources used for computing the three-dimensional (3-D) Moho interface. Tsuboi's technique (identical to the equivalent stratum theorem) is used here to map the 3-D Moho interface by selecting mean source depths from the results of the spectral analysis, and assuming a homogeneous density contrast of 350 kg/m³. The most characteristic feature of the 3-D Moho geometry was the presence of several lows associated with mountain ranges created by Alpine tectonics. In those areas, the gravity-derived Moho reaches a depth of up to 45 km in the Pyrenees and Cantabrian Mountains and close to 40 km under the Betics, Central System, and Iberian Chain. Under the Iberian Massif, the western part of the Iberian Peninsula composed of a Variscan basement, the Moho was located at a depth of 30–36 km. These results are consistent with existing seismic data and indicate that gravity-based techniques can provide very good estimates of lithosphere structure.

INTRODUCTION

Measurements of Earth's gravitational fi eld provide information on anomalous rock masses existing below the plane of observation. The basis for this is that the lithosphere is composed of heterogeneous rock masses that give rise to changes (i.e., anomalies) in gravity fields due to the density contrast in a given area. These anomalies are interpreted in terms of source geometries approximating geological structures at different depths. The basic problem associated with any gravity data interpretation technique lies in separating the contributions of shallow and deep sources. Such discrimination is accompanied by inherent ambiguity and uncertainty (Roy, 1962; Skeels, 1967) and questions the real validity of a technique for three-dimensional (3-D) Moho mapping. One of several mathematical methods of anomaly separation is based on the frequency contents of the observed data (Fuller, 1967; Zurflueh, 1967; Spector and Grant, 1970; Syberg, 1972). In general, shallow and deep sources are characterized by high- and low-frequency contents of the anomaly, respectively. Thus, the use of low-pass filters would seem to be a reasonably good technique to distinguish the contributions related to the Moho discontinuity/boundary from the observed anomaly. However, shallow bodies of significant lateral extension, such as sedimentary basins, may not be fully removed by low-pass filtering (Chakraborty and Agarwal, 1992). The existence of lateral density variations within the crust introduces further uncertainties for separating anomalies. Spectral analysis (Spector and Grant, 1970; Syberg, 1972) has been used to estimate the average depths of sources occurring at different levels, which is required to compute the Moho relief. The inversion techniques available in the literature are suitable for isolated source geometries only (Nabighian et al., 2005).

In this study, we used gravity data for the Iberian Peninsula to map the Moho. The Ibe-rian Peninsula features sharp contrasts in crust thickness between its Alpine and Variscan tec-tonic units. The approach used was a simple yet efficient method proposed by Tsuboi (1979) to invert low-pass-filtered anomalies associated with the gravity Moho discontinuity under the assumption of a layered Earth model. Chakraborty and Agarwal (1992) and Agarwal et al. (1995) successfully demonstrated the utility of long-wavelength anomalies in crustal studies. For example, this technique has been successfully used to map the Moho under complex geological structures across France and adjoining regions (Lefort et al., 1998; Lefort and Agarwal, 1999, 2000, 2002). The Moho map produced here shows a relief pattern similar to seismic-derived Moho maps while avoiding dubious interpretations due to a lack of seismic data. Effectively, our results indicate that gravity-based methods are powerful tools to determine the structure of the continental crust.

GEOLOGICAL SETTING AND CRUSTAL THICKNESS

Continental Iberia can be divided into a west-ern part consisting of Paleozoic and Proterozoic rocks and an eastern part in which Mesozoic and Cenozoic sediments predominate (Fig. 1). The western part, or Iberian Massif, is a fragment of the Variscan orogen composed of metamorphic and igneous rocks. The Iberian Massif features several tectono-stratigraphic zones, some of which are bounded by sutures that represent the diverse microcontinents involved in the oblique collision among Gondwana, Laurentia, and Baltica in the Paleozoic (Matte, 1991). Once the Variscan cycle was over, the geodynamic evolution of the Iberian plate was controlled by the Tethys cycle and opening of the North Atlantic (Capote et al., 2002; Ribeiro, 2006). In the early Mesozoic, the Iberian plate was deformed by large-scale stretching, which gave rise to extensional basins at the Iberian plate margins and within the intraplate domain. The

present geology of the Iberian Peninsula was shaped from the Late Cretaceous to late Cenozoic when the European and African plates converged. Intense crustal deformation took place at the Iberian plate margins. At the northern boundary, an E-W mountain chain—the Pyrenean belt—developed as a collisional orogen verging both to the N and S and extending from the Mediterranean Sea to the Atlantic Ocean. Within this belt, there are two ranges, the Pyrenees to the east and the Cantabrian Mountains to the west (Fig. 1). The southern margin of the belt is defined by two foreland basins, the Duero and the Ebro Basins, which formed by infilling sediments as a result of erosion related to the uplifted orogen. At the southern margin of the Iberian plate, convergence of the African and Iberian plates formed the Betics. The flexural response of the lithosphere created the Guadalquivir Basin, which has been infilled with Neogene to Quaternary rocks, at the northern margin of the Betics. Since the middle-late Miocene, the orogen has undergone severe extensional deformation inducing crustal thinning (Comas et al., 1992; Torné and Banda, 1992).

Within the Iberia intraplate domain, two mountain chains, the Iberian Chain and Central System, developed in the Cenozoic. The Iberian Chain in the east consists of thick sequences of Upper Permian to Mesozoic sediments. The Central System trends NE-SW along the central part of continental Iberia. It consists of an uplifted crustal block bounded by two main reverse faults determining that basement rocks overlie Tertiary sediments of the Duero and Tajo Basins.

Crustal Thickness

A Bouguer anomaly map of the Iberian Peninsula (Mezcua et al., 1996) reflects crustal thickness differences and negative anomalies related to crustal roots. The gravity Moho map of De Vicente (2004; Fig. 7b) assumed an Airy-Heiskanen model of isostatic equilibrium, and also displayed a thickened crust under the Alpine chains, but in general depths were lower than those estimated from the seismic studies mentioned next. On the Mediterranean coast, the Moho has been located at 24 km (e.g., Dañobeitia et al., 1992; Gallart et al., 1994) and reaches a depth of ~28 km at the Atlantic margin (e.g., Córdoba et al., 1987; González et al., 1998; Díaz et al., 2003). The Pyrenees, in the Alpine Ranges, exhibit among the largest crust thicknesses. Beneath its axial zone, the Moho deepens to 45–50 km (Daignieres et al., 1998; Choukroune and ECORS Team, 1989), while to the east, toward the Mediterranean coast, the Moho rises to ~24 km. The thickened crust extends to the west beneath the Cantabrian Mountains, where the Moho attains a depth of 46–48 km (Pulgar et al., 1996; Fernández-Viejo et al., 1998, 2000; Díaz et al., 2003). Seismic data for the other major Alpine chains, i.e., the Betics, reveal a crust of ~32 km at the margins, increasing further toward the central zone to ~36–38 km. The crust progressively thins toward the southern margin of the Betics, and the Moho rises to a depth of ~15 km in the Alboran Sea (Fig. 1) (Hatzfeld and Ben Sari, 1977; Working Group for DSS in the Alboran Sea, 1974, 1978). For the Iberian Chain, a crustal thickness of 40 km derived from gravity studies (Salas and Casas, 1993) is consistent with the seismic profile interpretation (Zeyen et al., 1985; Gallart et al., 2004). The Moho has been attributed a maximum depth of 35 km under the Central System, shallowing to ~30 km under the Duero and Tajo Basins (Suriñach and Vegas, 1988; ILIHA DSS Group, 1993). In the western and central parts of the Iberian Peninsula, Moho depth varies from 30 to 34 km under the Iberian Massif and the Tertiary basins (Banda

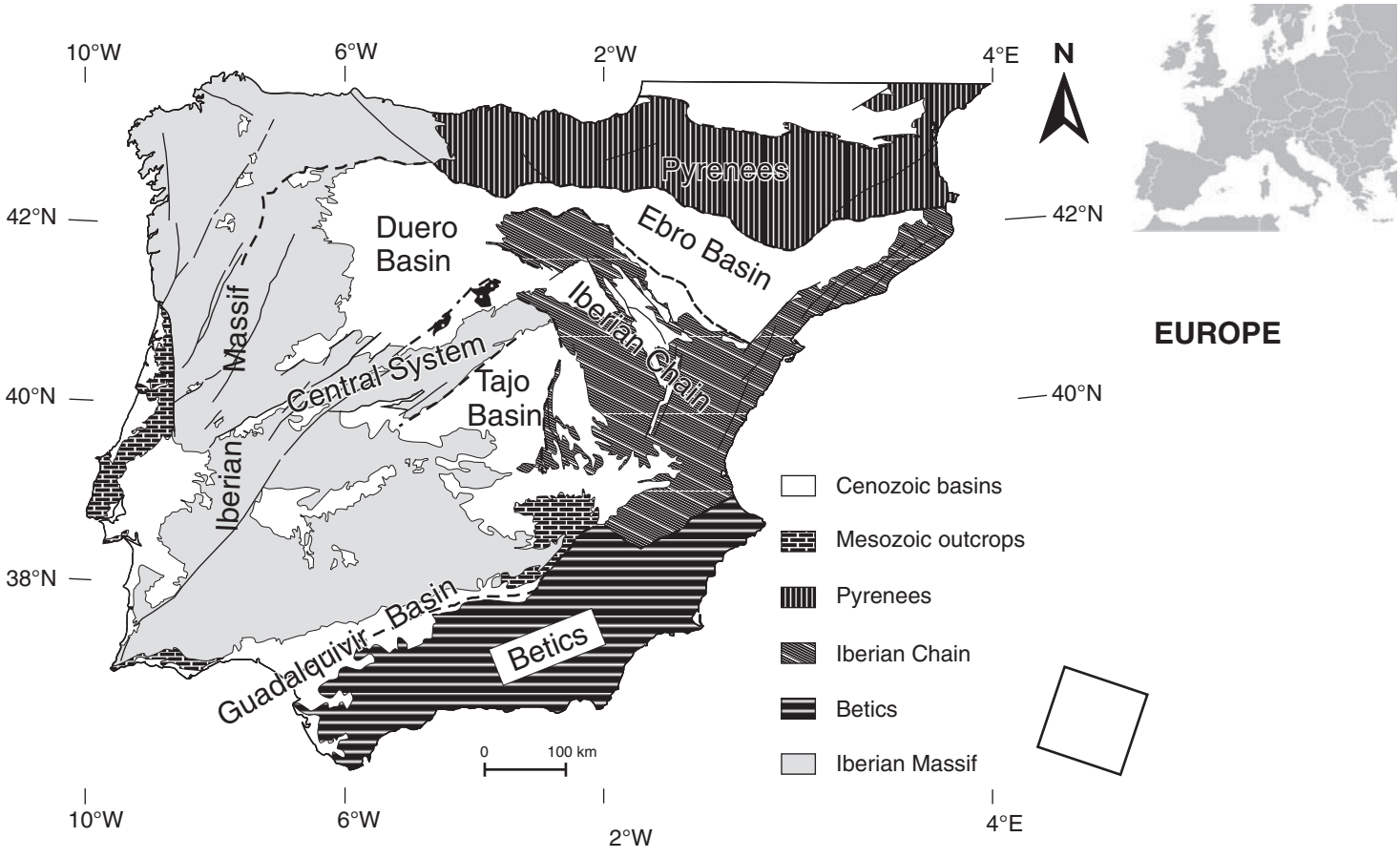

Figure 1. Geological map of the Iberian Peninsula.

et al., 1981; Córdoba et al., 1987; ILIHA DSS Group, 1993; Téllez et al., 1993; Gallart et al., 1994; Pulgar et al., 1996; González et al., 1996, 1998; Flecha et al., 2009).

ANALYSIS OF THE GRAVITY ANOMALIES

Gravity Data

Three different sets of gravity data were combined to construct a final anomaly map. The first data set, obtained by the present authors, includes data from 2892 gravity stations covering an area of ~23,657 km^2 in central Spain (Fig. 2). All gravity measurements were corrected for Earth-tide, free-air, and Bouguer effects. Terrain correction up to 166.7 km was also applied. Terrain correction was applied by considering topography variation up to a radius of 166.7 km from the point of observation. In addition, we used 28,202 data points from the Bouguer anomaly map of the Iberian Peninsula (Mezcua et al., 1996), and data from the Bureau Gravimetrique Internationale (BGI) for France (141,223 stations) to the north, and Morocco and Algeria (8613 stations) to the south. A comparison of 469 duplicate gravity measurements revealed a root mean squares error of ±0.88 mGal. This is an acceptable error for a regional study, and thus the different data sets were merged. A standard density value of 2670 kg/m^3 was used in the reduction of the data. For gravity values in marine areas, the most detailed bathymetric data available were used to compute the Bouguer anomalies from the free-air gravity anomalies (GEODAS database from the National Geophysical Data Center, http://www.ngdc.noaa.gov/mgg/geodas/geodas.html). This was done by replacing the seawater with a slab of density 2670 kg/m^3 and thickness equal to the bathymetric depth determined using the GEBCO Digital Atlas data (IOC, IHO, and BODC, 2003) available for the area. The last of the three data sets used,

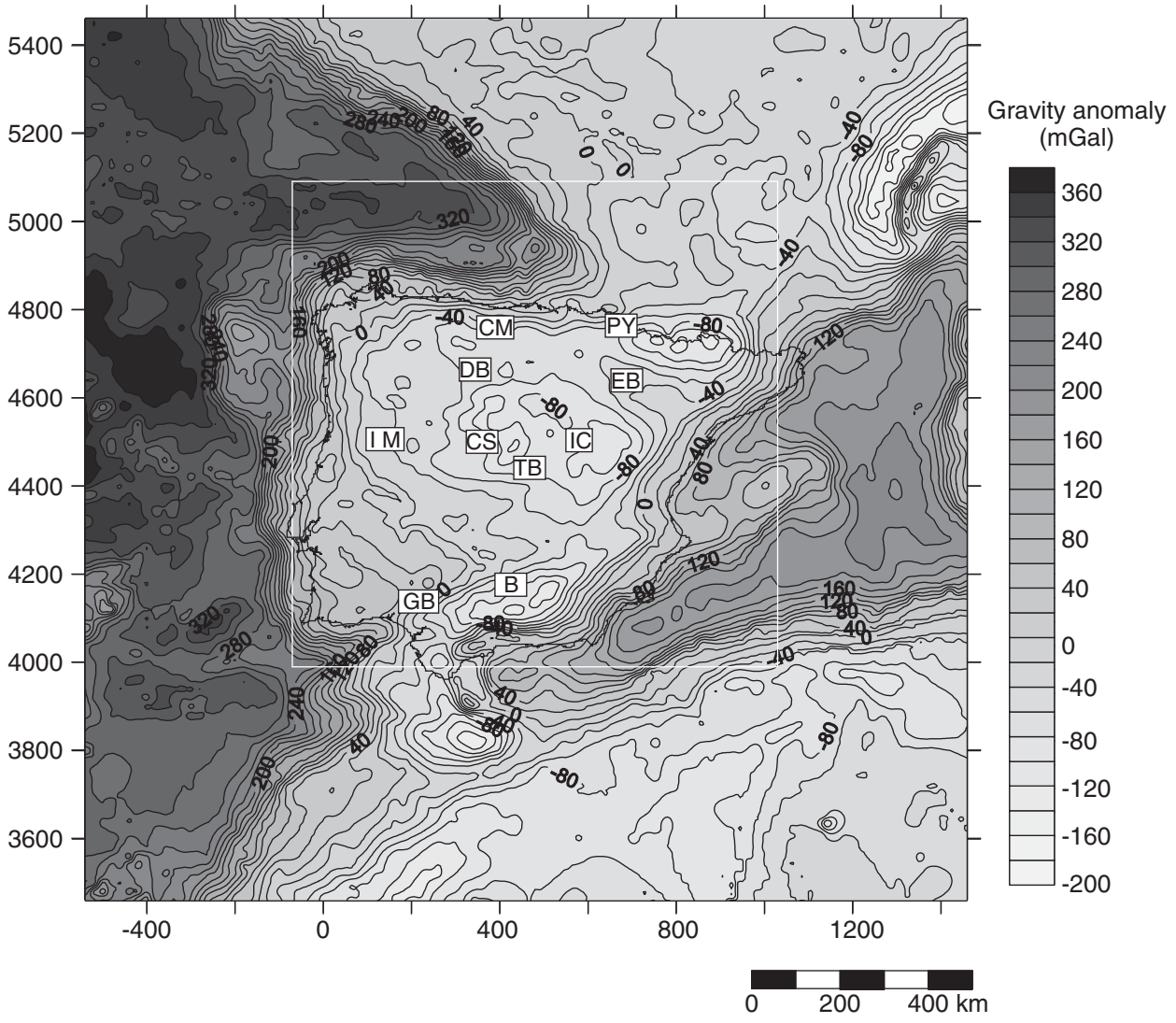

Figure 2. Bouguer gravity anomaly map of the Iberian Peninsula and surrounding areas. UTM coordinates in kilometers, zone 30N. Inset shows the central area retained after data processing and analysis. The abbreviations used are: CM—Cantabrian Mountains; PY—Pyrenees; DB—Duero Basin; EB—Ebro Basin; CS—Central System; TB—Tajo Basin; IC—Iberian Chain; GB—Guadalquivir Basin; B—Betics; IM—Iberian Massif.

corresponding to an offshore area, included data recorded at 9400 stations.

The station data were interpolated by kriging with a spacing of 5 km and a total length of 2000 km both in *x* and *y* directions (grid size: 401 rows by 401 columns) to generate a Bouguer anomaly map (Fig. 2), which was then subjected to spectral analysis, low-pass filtering, and inversion. After this processing, only the central core corresponding to the Iberian Peninsula (1500 km × 1140 km) was retained and displayed for minimization of artifacts due to Fourier transform–based data processing techniques.

Figure 2 shows that the gravity field over the entire area varies from −200 to +378 mGal, and over the Iberian Peninsula, it varies from −140 to +220 mGal. Relatively large negative anomalies may be observed across the continental areas of the Iberian Peninsula. The marine part of this peninsula displays positive anomalies associated with crustal thinning in a seaward direction from the coast. Figure 2 generally exhibits good correlation with geological units. The Alpine chains are associated with gravity anomaly minima. Prior gravity and seismic studies indicate that the main cause of these anomalies is a thickened crust (e.g., Salas and Casas, 1993; Suriñach and Chavez, 1996; Casas et al., 1997; Gómez-Ortiz, 2001; Rivero et al., 2002; Gómez-Ortiz et al., 2005). Gravity anomaly minima have also been linked to the Tertiary Duero and Tajo Basins. Positive anomalies observed in SW Iberia are due to increased crustal density toward the SW part of the Iberian Massif (Fig. 1); this density peaks in the Sub-Portuguese zone (e.g., Sánchez Jiménez, 2003).

Data Processing Techniques

The observed gravity anomaly is the sum of the contributions due to lateral variations in density within several lithological units, from the plane of observation to deep inside Earth. It is, therefore, essential to identify contributions due to lateral variations in density occurring at different depths. As a rule of thumb, high-frequency components of the observed anomalies are attributed to shallow depths, and low-frequency components are attributed to deep depths. Zurflueh (1967) suggested the use of appropriate low-pass filters to separate effects due to deep and shallow sources. A certain amount of uncertainty in achieving the anomaly contribution associated with a particular layered structure is likely to exist by the use of low-pass filters. We tackled this problem by extending the survey area by several hundred kilometers all along the area of interest.

Design of the Low-Pass Filter

A two-dimensional low-pass filter with a circularly symmetric frequency response having a prespecified low cutoff frequency was designed using the filter coefficients computed for a one-dimensional (1-D) data set. Martin (1962) described an excellent approach to computing digital filter coefficients of a low-pass filter with a prespecified cutoff frequency using a closed mathematical equation involving a prespecified roll off (transition zone) over which the amplitude response decreases as per the assumed mathematical function. These 1-D filter coefficients were then used in the space domain to yield coefficients for a 2-D filter by McCllelan transformation (McCllelan, 1973). Thus, we can easily compute a 2-D filter coefficient corresponding to any prespecified cutoff frequency and roll off.

Energy Spectrum Analysis

Spector and Grant (1970) proposed a statistical technique based on the ensemble average of the random distribution of anomalous sources below the plane of observation by computing the energy density of the observed data. These authors observed that a plot of the natural logarithm of the energy of the anomaly versus angular frequency exhibits a decay in energy produced with increasing angular frequency. Syberg (1972) mathematically proved that the decay process is predominantly controlled by the ensemble average depth of the random distribution of sources, which can be approximated by straight lines (e.g., corresponding to regional and residual anomalies). Thus, the power spectrum may be expressed in terms of straight-line segments characterizing the sources at different depth levels. When this study is performed over a large area, the averaged depths will be related to the main density discontinuities of the lithosphere. Because there is a relationship between density and P-wave velocity, we can correlate the lithospheric P-wave velocity discontinuities with the Moho.

Computing the Mass Distribution and Relief of an Interface

We used Tsuboi's (1979) technique to compute mass distribution, which was then converted into Moho relief. The details of the mathematical formulation used can be found in the Appendix. The basic assumptions considered for computing the relief in Moho depth are: (1) the gravity effect (anomaly) is entirely due to the relief at the interface formed by two isotropic and homogeneous rocks of different densities, and (2) the density contrast and mean depth to the horizontal interface are known.

Processing of Gravity Data

The gravity anomaly map (Fig. 2) reveals high-frequency "noises" superimposed on the main anomaly trends. These noises represent an unwanted signature to be removed before any discussion of the data. To remove the high-frequency component, the observed data matrix (401 × 401 points) was low-pass filtered to allow the passage of only those anomalies associated with a wavelength of 40 km and above. Such an approach minimizes aliasing, and computation of the energy spectrum becomes more reliable. The filtered map (not shown here) after removal of the noise was used as the base map for further data processing and analysis.

To study the probable depths of the sources, the entire matrix of observed data (Fig. 2) was subjected to the 2-D Fast Fourier Transform algorithm to plot the logarithm of the energy of anomalies versus angular radial frequency (Fig. 3). Three linear segments were distinguished in this plot, each of which is associated with a range of frequencies, providing an indication of their average depth. The depths of the anomalous horizons are: 134, 25.6, and 10.9 km. From other independent geophysical information, we can relate these horizons to main crustal discontinuities. Several recent publications (e.g., Piromallo and Morelli, 2003; Boschi et al., 2004; Panza et al., 2007; Fullea et al., 2010) dealing with mantle structure in the Iberian Peninsula inferred from shear-wave tomography and P-wave velocity data have located the lithosphere-asthenosphere boundary (LAB) at a depth of 110–140 km. Our deepest depth is fairly consistent with this estimate, suggesting it could correspond to the base of the lithosphere. Our intermediate-depth value represents a mean Moho depth for the study area, taking into account marine and continental areas (see section on geological setting and crustal thickness). The shallowest depth could be located within the crust and could represent a major crust discontinuity like the upper crust–lower crust boundary (e.g., ILIHA DSS Group, 1993; Suriñach and Vegas, 1988; González et al., 1998; Simancas et al., 2003).

Through several studies (Lefort and Agarwal, 1996, 1999, 2000, 2002) using small and large data sets, it has been observed that a low-pass-filtered anomaly map with a cutoff wavelength around 150 km will effectively correspond to Moho anomalies. Though this cutoff wavelength may vary from area to area with variations in the geological setup, the computed Moho depth needs to be compared with seismic data to assess

the quality of the outcome. The low-pass-filtered anomaly map (Fig. 4) obtained from the data in Figure 2 for wavelengths greater than 150 km is quite smooth, and it is likely to reflect anomalies associated with the Moho discontinuity.

We further computed the topographic relief of the Moho discontinuity (Fig. 5) in Figure 4 using Tsuboi's (1979) method, by assuming a mean depth to a horizontal interface of 25 km, obtained from the spectral analysis (h2, Fig. 3). From published crustal layer velocities and the P-wave velocity–density empirical relationship (Christensen and Mooney, 1995), a mean density contrast of 350 kg/m^3 between crust and mantle is estimated.

GRAVITY MOHO MAP OF THE IBERIAN PENINSULA

The two largest Moho lows occur along the Pyrenees and Cantabrian Mountains, and the Betics. The first one runs parallel to the mountain belt, along the northern margin of the Iberian Peninsula trending E-W with deepening of the Moho to 45 km (Figs. 5 and 6, profiles 1 and 2). The second one trends ENE-WSW beneath the Betics. In the peninsula interior, two further Moho lows are respectively related to the Central System, trending NE-SW, and the Iberian Chain, trending NW-SE (Figs. 1 and 5). In the latter, the Moho reaches a depth of ~40 km. Far from the Alpine ranges, the gravity Moho shows a mean depth of 34 km, which decreases to 28–30 km toward the coast.

A relief map of seismic Moho depths averaged over a large area (0.5° × 0.5°) prepared by Díaz and Gallart (2009) reveals the existence of deep crustal roots under the Pyrenean Belt, as well as thickening of the crust under the Iberian Chain, Central System, and Betics (Fig. 6). Thus, due to averaging, the seismic Moho is much smoother than the computed gravity Moho. For a more detailed comparison between seismic Moho data and our gravity Moho, we constructed three profiles by integrating geological, seismic, and gravity data (Fig. 7). The northern part of profile 1 was close to the ECORS Central Pyrenees cross section (Choukroune and ECORS Team, 1989; Muñoz, 1992), and the Moho depths beneath the Iberian Chain were provided mainly by Zeyen et al. (1985) and Gallart et al. (2004). Profiles 2 and 3 were constructed by integrating the ESCIN-2 data in profile 2 and refraction and wide-angle reflection profiles in profiles 2 and 3 (Pulgar et al., 1996; Fernández-Viejo et al., 2000; Pedreira et al., 2003). In the southern areas of these profiles, seismic Moho depths under the Betics were taken from a deep seismic-reflection, seismic-refraction, and wide-angle reflection survey undertaken close to profile 3 (García-Dueñas et al., 1994; Banda et al., 1993). Moho depths under the Iberian Massif were compiled from seismic-refraction studies (ILIHA DSS Group, 1993; González et al., 1998) and seismic-reflection profiling (Simancas et al., 2003; Carbonell et al., 2007; Tejero et al., 2008). Seismic Moho depths beneath the Central System are those reported by Suriñach and Vegas (1988). Profile 1 (Fig. 7) reveals a good match between the seismic and gravity Moho in the Pyrenees and Iberian Chain. Both are characterized by well-defined gravity lows produced mainly by a thickened crust (Zeyen et al., 1985; Salas and Casas, 1993; Gallart et al., 2004). The greatest mismatches are found in the Cantabrian Mountains and the Betics. Under the Cantabrian Mountains, the gravity Moho shallows to 38 km, while seismic data indicate a depth of 45 km (Fig. 7, profiles 2 and 3). In this region, the gravity anomaly is characterized by a smooth gravity low bounded by the positive anomalies extending eastward far from the coast (Fig. 2). These discrepancies in Moho depths correspond to an area of crustal doubling due to convergence processes. In the south of the Iberia margin, under the Betics, the gravity Moho is ~5 km deeper than the seismic Moho (~36 km) (Figs. 1 and 7, profiles 2 and 3). In this Alpine chain, even different seismic methods have yielded different Moho depths. Seismic tomographic imaging suggests a 34–36-km-thick crust, in contrast to seismic-reflection estimates of 28–30 km beneath the topographic highs (García-Dueñas et al., 1994; Carbonell et al., 1998). Magnetotelluric studies have suggested the presence of a large conductive layer interpreted as a zone of partial melting within the lithosphere (e.g., Carbonell et al., 1998). This would decrease the density of the lithospheric mantle, increasing the gravity minimum associated with the Betics and deepening the calculated gravity Moho. The gravity Moho indicates a thicker crust than the seismic Moho (40 km versus 34 km) under the Central System. This discrepancy may be due to superimposition of gravity effects of low-density Tertiary sediments of the Duero and Tajo Basins on the effects of the crustal root of the Central System. Both these factors are considered to be responsible for the gravity minimum in the central part of the Iberian Peninsula.

The gravity Moho varies from 28 to 36 km in the Iberian Massif, where seismic surveys have indicated a depth of 30–35 km (ILIHA DSS Group, 1993; Díaz and Gallart, 2009; Palomeras et al., 2009) and a decrease in crustal

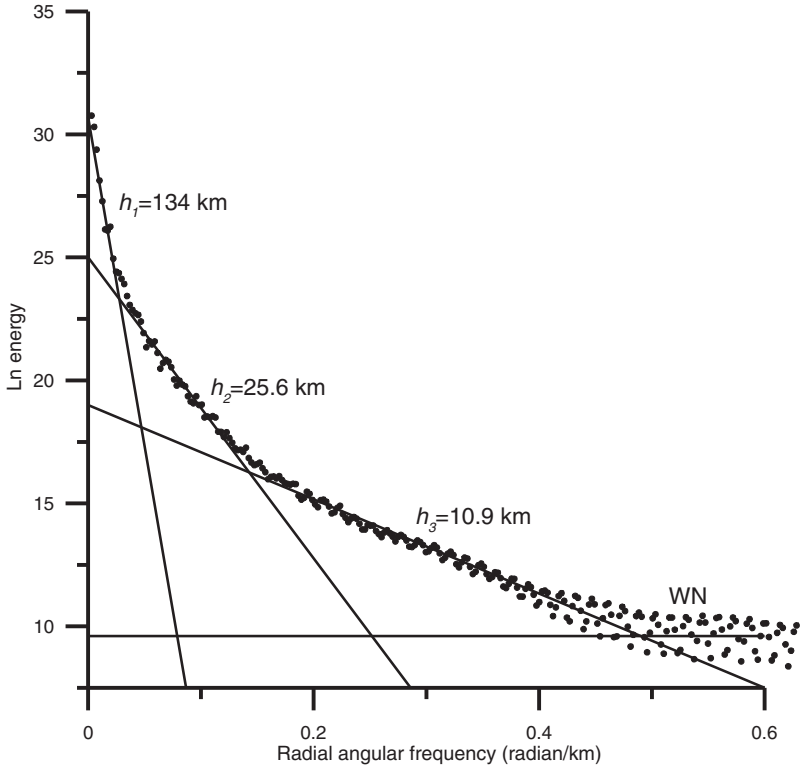

Figure 3. Plot of the logarithm of the power of Bouguer anomaly versus radial angular frequency. Three linear segments, corresponding to causative sources located at mean depths of 134, 25.6, and 10.9 km, are matched. WN—white noise.

thickness of only ~3 km southwestward in the Sub-Portuguese zone (Matias, 1996). Seismic surveys in the SW Iberian Peninsula have revealed that the seismic signature of the crust changes laterally (ILIHA DSS Group, 1993; González et al., 1996). Recently, Flecha et al. (2009) took into account the heterogeneous character of the crust and obtained more realistic average velocity models considering a high-velocity layer at midcrustal depth, a highly reflective lower crust, and a relatively horizontal Moho. The resulting model exhibits a layered mafic intrusion in the middle crust, which had been previously identified through seismic-reflection profiling (Simancas et al., 2003; Carbonell et al., 2007), and a strongly laminated lower crust with a Moho depth of ~33 km.

DISCUSSION AND CONCLUSIONS

The previous comparisons indicate maximum differences in depth between seismic and gravity Moho estimates ranging from 5 to 10 km, and they are concentrated in areas of crustal doubling, where the short wavelength of the Moho crustal root cannot be recovered by the filtering technique applied to the gravity data. Apart from this, the discrepancies between both Moho maps are not significant due to the fact that they fall into the uncertainty values inherent to both methods (Fig. 7). Indeed, seismic-derived Moho depths also have several uncertainties in interpretation leading to variations from ±2 to ±10 km in depth (e.g., Grad et al., 2009), which are associated with determination of velocities in different horizons and type of the seismic method used to estimate the depth (e.g., modern seismic-refraction profiles, surface wave tomography, reflection surveys, broadband stations, etc.). Significant numbers of refraction and reflection lines have sampled the crust of the Iberian Peninsula lithosphere and have reported crustal thicknesses and P-wave velocities. Published results for the same area present Moho depth variations close to ±3 km (Díaz and Gallart, 2009, and references therein). For example, the Moho depth map of Figure 6 displays a Moho located 2 km shallower in the central Iberian Peninsula in comparison to data profiling (Suriñach and Vegas, 1988). This effect corresponds to gridding smoothing. Thicknesses estimated from Vp/Vs ratio

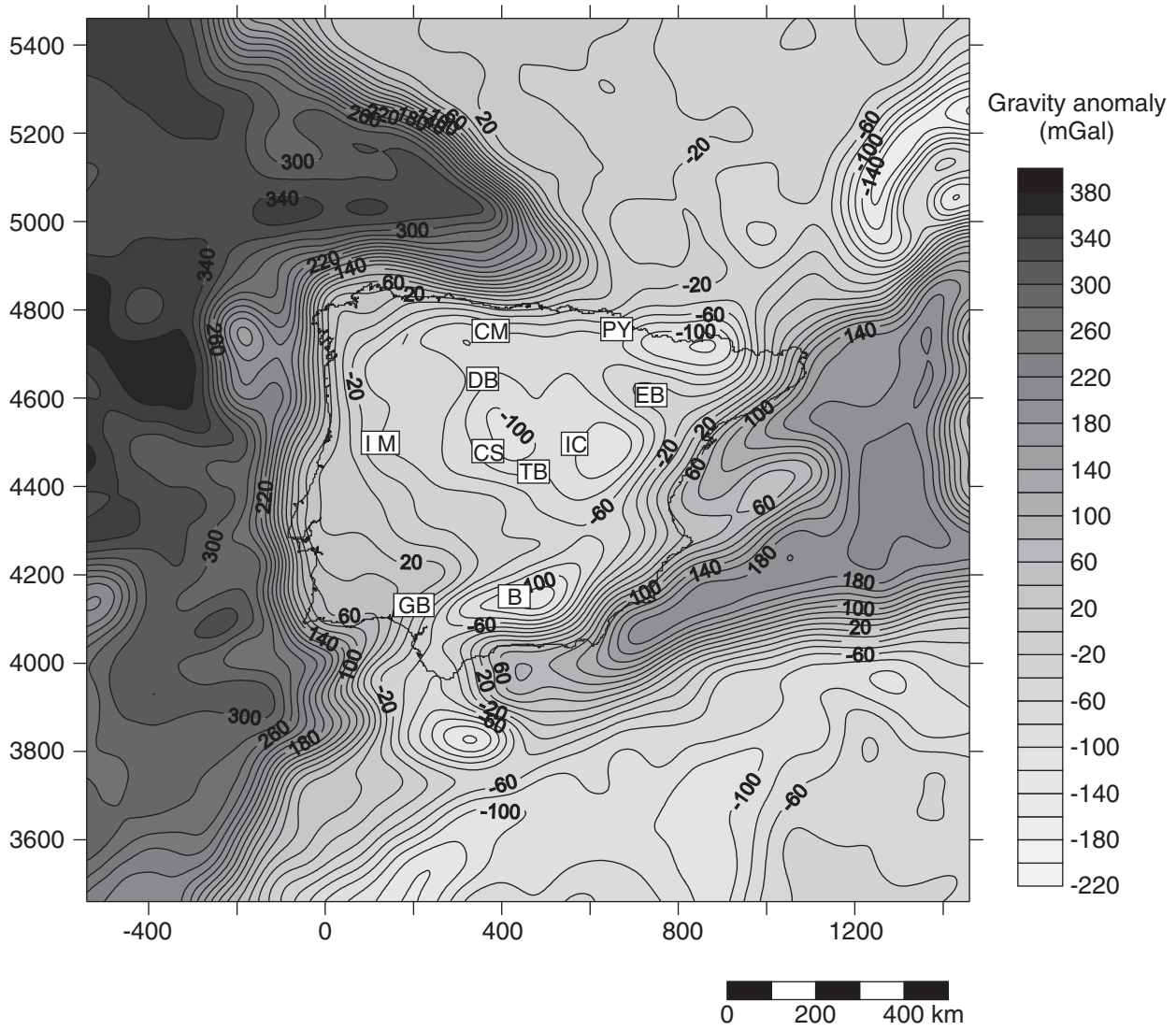

Figure 4. Filtered gravity anomaly map created to retain wavelengths greater than 150 km corresponding to Moho undulations in the Iberian Peninsula and surrounding areas. UTM coordinates in kilometers, zone 30N. Abbreviations are as in Figure 2.

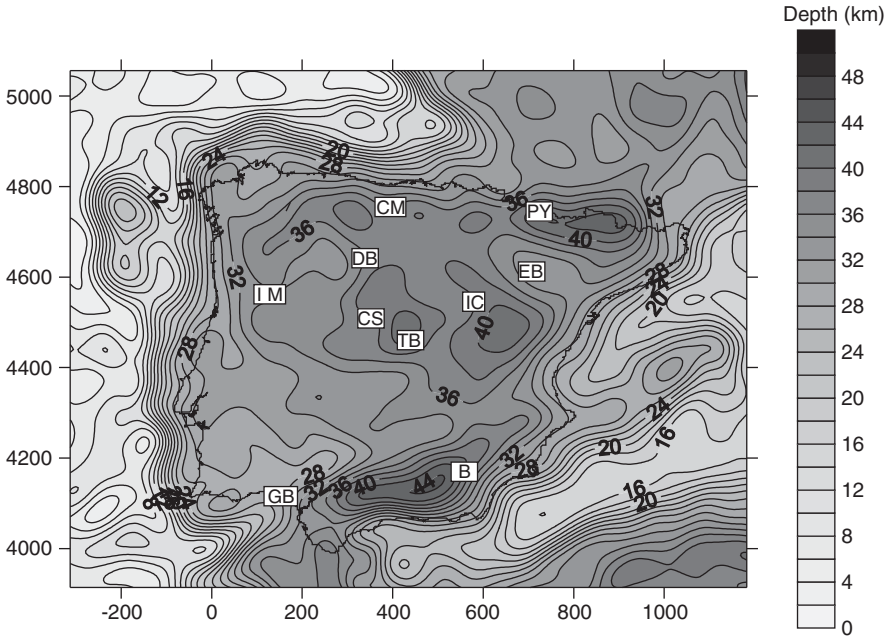

Figure 5. Gravity Moho depth map obtained by inverting the filtered gravity anomaly of Figure 4 using Tsuboi's (1979) method. UTM coordinates in kilometers, zone 30N. Abbreviations are as in Figure 2.

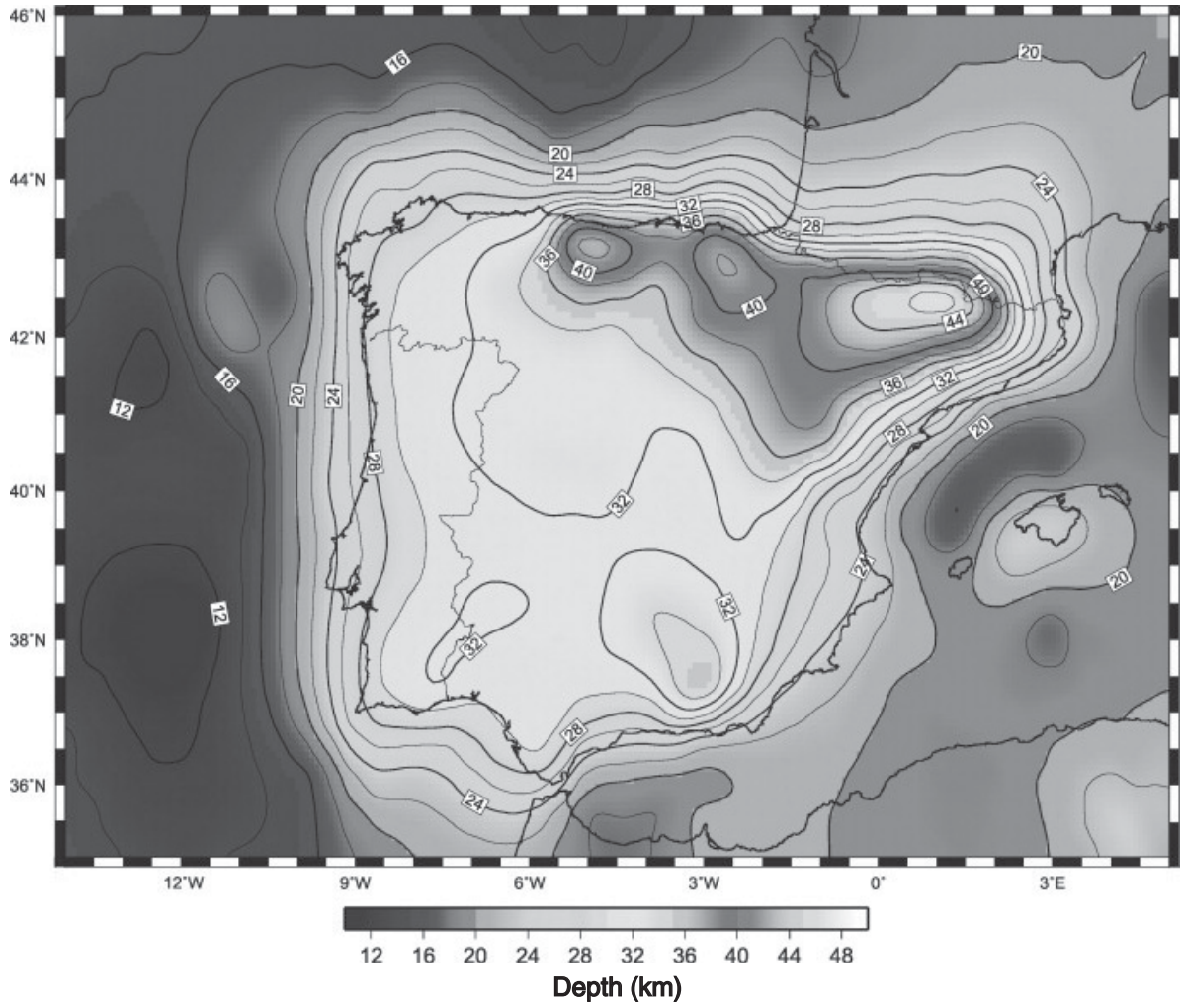

Figure 6. Interpolated seismic crustal depth model for the Iberian Peninsula. Crustal thickness isolines represented every 2 km. Figure is reprinted with permission from Elsevier from Diaz and Gallart, "Crustal structure beneath the Iberian Peninsula and surrounding waters: a new compilation of deep seismic sounding results," *Physics of the Earth and Planetary Interiors*, v. 173, p. 181–190, copyright 2009.

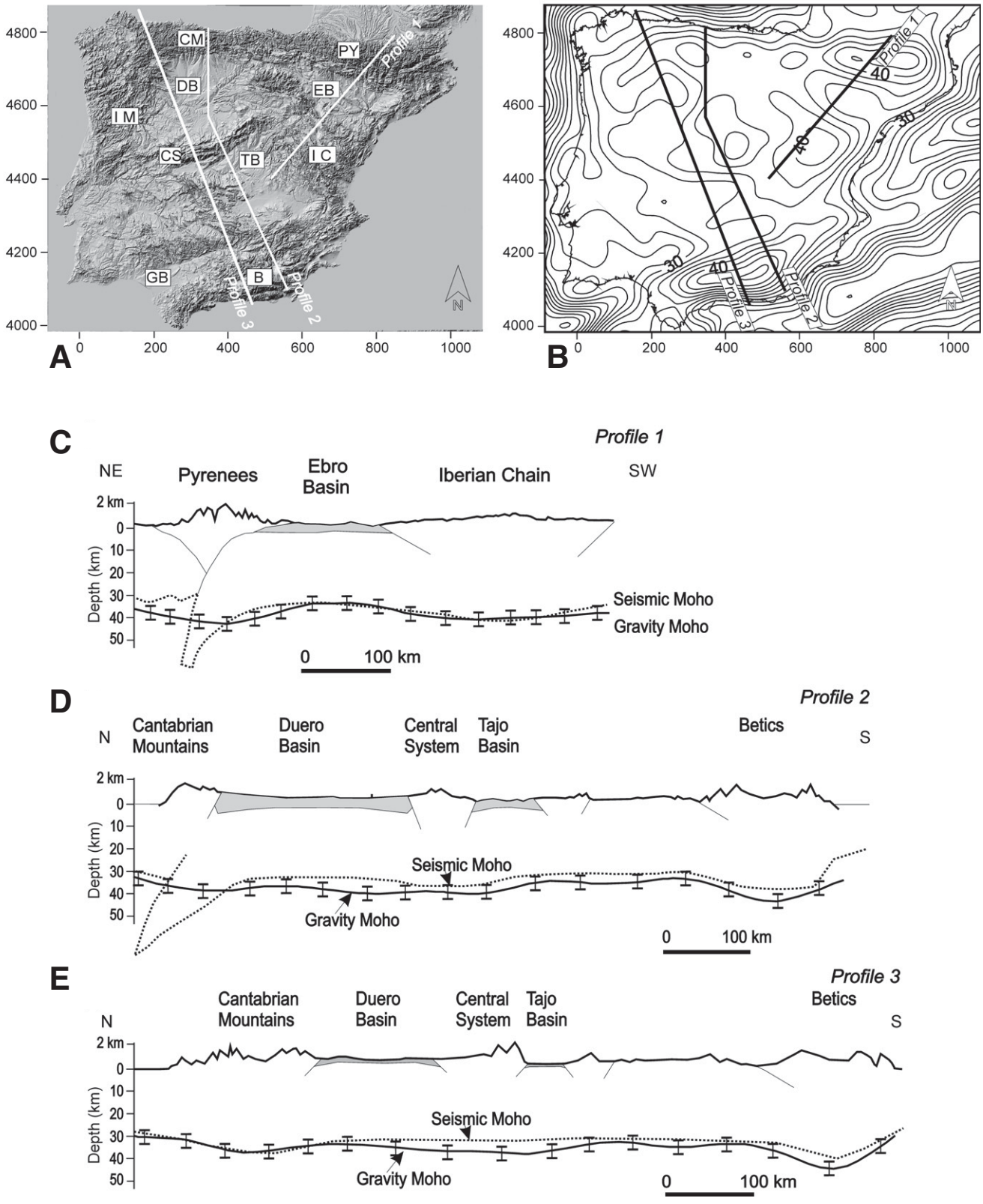

Figure 7. (A) Topography of continental Iberia and (B) gravity Moho depth contours showing the location of three profiles (C, D, and E) used to illustrate the relationship between seismic and gravity Moho depths. UTM coordinates in kilometers, zone 30N. Large Moho depths are associated with Alpine ranges. Abbreviations are as in Figure 2. Error bars represent the uncertainty value estimated for the Moho gravity data.

variations show uncertainties ranging from ±0.5 to ±2.5 km (Julià and Mejía, 2004). These values are similar to those obtained from other seismic methods. Thus, we can conclude that an uncertainty of seismic Moho depth of ±3–4 km can be assumed in the Moho depth data for this area. In contrast, errors in computed gravity Moho depths are mainly the consequence of inadequate separation between shallow and deep sources, uncertainties on prespecified cutoff wavelength, density contrast, and assumed mean depth of the interface. Also, long wavelengths due to shallow sources such as Tertiary basins may affect the computed depth of the anomalous horizon. Gómez-Ortiz et al. (2005) argued that if the effect of shallow sources is removed, the mean depth regional source is better defined. This could be very important when the study area is relatively small and long-wavelength shallow sources are sufficiently large to mask the effect of deep sources. The density contrast value used here is derived from seismic velocities and the cutoff wavelength can be determined from the gravity power spectrum or can be assumed from previous works. Here, we assumed a cutoff wavelength of 150 km, which was successfully applied to analyze the gravity data over a crust with characteristics close to those of the Iberian Peninsula. In order to visualize the uncertainty involved in computation of Moho depth from gravity data, we obtained different Moho depth maps by varying density contrast and Moho mean depth values. The density contrast and mean depth data values were 350 ± 30 kg/m^3 and 25 ± 2 km, respectively, which are considered representative for the studied area. Using all the maps generated, the root mean square (RMS) error was obtained as an estimation of the uncertainty in Moho depth due to variations in the two key parameters used during the inversion of gravity data. The resulting uncertainty is ±3.1 km, similar to the seismic uncertainty previously mentioned. This value has been incorporated into the Moho profiles (Fig. 7) in the form of error bars for comparison with the corresponding seismic Moho data. Thus, we consider that the generated gravity Moho map adequately represents the relief of the base of the Iberian crust and that the techniques used demonstrate their robustness to estimate main density discontinuity depths and topography.

The following main conclusions may be drawn from our study.

Through two-dimensional filtering and spectral analysis of available gravity data for continental Iberia, we were able to identify three main anomalous horizons within the lithosphere at depths of 134, 25.4, and 10.9 km. Geophysical data suggest that these correspond to the lithosphere-asthenosphere boundary, Moho discontinuity, and the upper-lower crust limit, respectively.

(1) The major characteristic feature of the gravity derived 3-D Moho geometry is the presence of several lows associated with mountain ranges created during Alpine tectonics. In these areas, the gravity Moho reaches a depth of up to 45 km in the Pyrenees and Cantabrian Mountains and close to 40 km under the Betic Ranges, Central System, and Iberian Chain. Under the Iberian Massif, the western part of the Iberian Peninsula composed of a Variscan basement, the Moho was located at a depth of 30–36 km.

(2) Our results are similar to seismic data, suggesting that the present technique can provide a reasonable estimate on depths of the lithospheric discontinuities.

ACKNOWLEDGMENTS

Agarwal acknowledges the Department of Science and Technology, Government of India, New Delhi, for funding several projects having objectives to improve the computational facilities used in the present work. Ruiz was supported by a Ramon y Cajal contract, cofinanced by the European Social Fund. We also thank Shalivahan Srivastava for revising the manuscript and for useful comments. We greatly appreciate the comments and suggestions of the associate editor (Donald White), Andrew Hynes, and an anonymous reviewer, that have considerably improved the original manuscript. We wish to thank Ana Burton for linguistic assistance. This research was supported by Ministerio de Ciencia e Innovación, Project CGL2008-03463.

APPENDIX

THEORY ON COMPUTATION OF MASS DISTRIBUTION

Let us assume a Cartesian system of coordinates with z-axis positive vertical downward. Let $f(x, y)$ be a certain quantity measured on the horizontal plane (x, y). We can express $f(x, y)$ by a double Fourier series of the form (Tsuboi, 1979)

$$f(x,y)=\sum_m\sum_n \alpha_{mn} \begin{matrix}\cos\\ \sin\end{matrix} mx \begin{matrix}\cos\\ \sin\end{matrix} ny. \quad \text{(A1)}$$

Suppose a distribution of $f(x, y)$ is given within a square $0 \le x \le 2\pi, 0 \le y \le 2\pi$. The distribution of the value of $f(x, y)$ in the direction of x along a certain value of y can be expressed by a single Fourier series of x such as

$$f(x,y)=\sum_m \beta_m(y) \begin{matrix}\cos\\ \sin\end{matrix} mx. \quad \text{(A2)}$$

The coefficient β_m changes according to y, so that it can be expressed by a single Fourier series of y such as

$$\beta_m(y)=\sum_m \gamma_n \begin{matrix}\cos\\ \sin\end{matrix} mx. \quad \text{(A3)}$$

Then as a whole, $f(x, y)$ is

$$f(x,y)=\sum_m\sum_n \beta_m\ \gamma_n \begin{matrix}\cos\\ \sin\end{matrix} mx \begin{matrix}\cos\\ \sin\end{matrix} ny. \quad \text{(A4)}$$

If $\beta_m\gamma_n$ is written as α_{mn}, then

$$f(x,y)=\sum_m\sum_n \alpha_{mn} \begin{matrix}\cos\\ \sin\end{matrix} mx \begin{matrix}\cos\\ \sin\end{matrix} ny. \quad \text{(A5)}$$

Using this double Fourier series, if a distribution of gravity values $g(x, y)$ is

$$g(x,y)=\sum_m\sum_n B_{mn} \begin{matrix}\cos\\ \sin\end{matrix} mx \begin{matrix}\cos\\ \sin\end{matrix} ny, \quad \text{(A6)}$$

then the underground mass M at a depth d that will produce this $g(x, y)$ is given by

$$M(x,y)=\frac{1}{2\pi G}\sum_m\sum_n B_{mn}\ \exp\{d\sqrt{(m^2+n^2)}\} \begin{matrix}\cos\\ \sin\end{matrix} mx \begin{matrix}\cos\\ \sin\end{matrix} ny. \quad \text{(A7)}$$

In the two-dimensional cases, the coefficients are 4 mn in number. For instance, if 2π is divided into six both in *x*- and *y*-directions, the number of coefficients will be 4 × 6 × 6 = 144, instead of 6 in one-dimensional case. If 2π is divided into 18, the number of coefficients needed are as many as 4 × 18 × 18 = 1296. The factor four is needed because there are four different combinations: cos *mx*·cos *ny*, cos *mx*·sin *ny*, sin *mx*·cos *ny*, and sin *mx*·sin *ny*.

The (sin *x*)/*x* method can also be extended to two-dimensional cases. In these cases, the integral,

$$\phi' = \int_0^1 \int_0^1 \cos mx \ \cos ny \ \exp\{d\sqrt{(m^2 + n^2)}\} dm \ dn, \qquad \text{(A8)}$$

has to be evaluated numerically for different values of *x* and *y*. It may be worth mentioning here that the coefficient ϕ' exhibits eightfold symmetry as observed in a downward-continuation filtering operation. There are several tables that give the values of ϕ' (Tsuboi et al., 1958; Kanamori, 1963; Takeuchi and Saito, 1964; all taken from Tsuboi, 1979) for various values of *d*. To apply this method to two-dimensional gravity interpretations, gravity values g_{mn} at square grid points and ϕ'_{mn} values at the corresponding points are multiplied, and the products $g_{mn}\phi'_{mn}$ at all the grid points are added. When the sum of all the products is divided by $2\pi G$, this will give the mass right beneath the point corresponding to $m = n = 0$. Here, *G* is universal gravitational constant. The relief in the interface at the point of computation can be obtained by dividing the computed mass by the density contrast Δρ between the upper and the lower formations.

The previous technique for computation of relief due to a single interface is exactly the same as proposed by Grant and West (1965) using the equivalent stratum theorem in the gravity field. Grant and West (1965, p. 250, their Equation 9.9 and fig. 9.7) have proved an equation for equivalent stratum theorem as

$$g(x, y, d) = 2\pi G\Delta\rho \quad h(x, y), \qquad \text{(A9)}$$

where $g(x, y, d)$ is the downward-continued gravity anomaly at a depth *d*, and $h(x, y)$ is the vertical departure of the interface at any point from its mean depth *d*. Thus, by continuing the residual (filtered) gravity anomaly on the plane of measurement downward to an assumed depth, *d*, one can construct an equivalent topographic surface provided the density contrast is known. Grant and West (1965, p. 251) further stated that "...Whether this gives a correct picture of the shape of the discontinuity (interface) will depend, of course, on how much of the residual gravity field does actually originate from that interface and whether a part of the effect has been removed with the regional trend."

REFERENCES CITED

Agarwal, B.N.P., Das, L.K., Chakraborty, K., and Sivaji, Ch., 1995, Analysis of the Bouguer anomaly over central India: A regional perspective: Memoir of the Geological Society of India, v. 31, p. 469–493.

Banda, E., Suriñach, E., Aparicio, A., Sierra, J., and Ruiz de la Parte, E., 1981, Crust and upper mantle structure of the central Iberian Meseta (Spain): Geophysical Journal of the Royal Astronomical Society, v. 67, p. 779–789.

Banda, E., Gallart, J., García-Dueñas, V., Dañobeitia, J.J., and Makris, J., 1993, Lateral variation of the crust in the Iberian Peninsula: New evidence from the Betic Cordillera: Tectonophysics, v. 221, p. 53–66, doi: 10.1016/0040-1951(93)90027-H.

Boschi, L., Ekström, G., and Kustowski, B., 2004, Multiple resolution surface wave tomography: The Mediterranean basin: Geophysical Journal International, v. 157, p. 293–304, doi: 10.1111/j.1365-246X.2004.02194.x.

Capote, R., Muñoz, J.A., Simón, J.L., (coord.), Liesa, C., and Arlegui, L., 2002. Alpine tectonics I: The Alpine system north of the Betic Cordillera, *in* Gibbons, W., and Moreno, T., eds., Geology of Spain: London, Geological Society, p. 367–398.

Carbonell, R., Sallares, V., Pous, J., Dañobeitia, J.J., Queralt, P., Ledo, J.J., and García Dueñas, V., 1998, A multidisciplinary geophysical study in the Betic chain (southern Iberia Peninsula): Tectonophysics, v. 288, p. 137–152, doi: 10.1016/S0040-1951(97)00289-8.

Carbonell, R., Simancas, F., Martínez-Poyatos, D., Ayarza, P., González, P., Tejero, R., Martín-Parra, L., Matas, J., González-Lodeiro, F., Pérez-Estaún, A., García-Lobón, J.L., Mansilla, L., and Palomeras, I., 2007, Seismic reflection transect across the Central Iberian zone (Iberian Massif): The Alcudia Project: Eos (Transactions, American Geophysical Union), v. 88, no. 52, Fall Meeting supplement, abstract T31B–0479.

Casas, A., Kearey, P., Rivero, L., and Adam, C.R., 1997, Gravity anomaly map of the Pyrenean region and a comparison of the deep geological structure of the western and eastern Pyrenees: Earth and Planetary Science Letters, v. 150, p. 65–78, doi: 10.1016/S0012-821X(97)00087-3.

Chakraborty, K., and Agarwal, B.N.P., 1992, Mapping of crustal discontinuities by wavelength filtering of gravity field: Geophysical Prospecting, v. 40, p. 801–822, doi: 10.1111/j.1365-2478.1992.tb00553.x.

Choukroune, P., and ECORS Team, 1989, The ECORS Pyrenean deep seismic profile reflection data and the overall structure of an orogenic belt: Tectonics, v. 8, p. 23–39, doi: 10.1029/TC008i001p00023.

Christensen, N.I., and Mooney, W.D., 1995, Seismic velocity structure and composition of the continental crust: A global view: Journal of Geophysical Research, v. 100, no. B7, p. 9761–9788, doi: 10.1029/95JB00259.

Comas, M.C., García Dueñas, V., and Jurado, M.J., 1992, Neogene tectonic evolution of the Alboran Basin from MCS data: Geo-Marine Letters, v. 12, p. 157–164, doi: 10.1007/BF02084927.

Córdoba, D., Banda, E., and Ansorge, J., 1987, The Hercynian crust in NW Spain: A seismic survey: Tectonophysics, v. 132, p. 321–333, doi: 10.1016/0040-1951(87)90351-9.

Daignières, M., Gallart, J., Hirn, A., and Surinach, E., 1998, Complementary geophysical surveys along the ECORS Pyrenees line: Mémoires de la Société Géologique de France, v. 173, p. 55–80.

Dañobeitia, J.J., Arguedas, M., Gallart, J., Banda, E., and Makris, J., 1992, Deep seismic configuration of the Valencia Trough and its Iberian and Balearic borders from extensive refraction-wide angle reflection seismic profiling: Tectonophysics, v. 203, p. 37–55, doi: 10.1016/0040-1951(92)90214-Q.

De Vicente, G., 2004, Estructura Alpina del antepaís Ibérico, *in* Vera, J.A., ed., Geología de España: Madrid, Spain, Sociedad Geologica de España-Instituto Geologico y Minero de España, p. 587–634.

Díaz, J., and Gallart, J., 2009, Crustal structure beneath the Iberian Peninsula and surrounding waters: A new compilation of deep seismic sounding results: Physics of the Earth and Planetary Interiors, v. 173, p. 181–190, doi: 10.1016/j.pepi.2008.11.008.

Díaz, J., Gallart, J., Pedreira, D., Pulgar, J.A., Ruiz, M., López, C., and González-Cortina, J.M., 2003, Teleseismic imaging of the Alpine underthrusting beneath N Iberia: Geophysical Research Letters, v. 30, no. 11, p. 1–4, doi: 10.1029/2003GL017073.

Fernández-Viejo, G., Gallart, J., Pulgar, J.A., Gallastegui, J., Dañobeitia, J.J., and Córdoba, D., 1998, Crustal transition between continental and oceanic domains along the North Iberian margin from wide angle seismic and gravity data: Geophysical Research Letters, v. 25, no. 23, p. 4249–4252, doi: 10.1029/1998GL900149.

Fernández-Viejo, G., Gallart, J., Pulgar, J.A., Córdoba, D., and Dañobeitia, J.J., 2000, Seismic signature of Variscan and Alpine tectonics in NW Iberia: Crustal structure of the Cantabrian Mountains and Duero basin: Journal of Geophysical Research, v. 105, p. 3001–3018, doi: 10.1029/1999JB900321.

Flecha, I., Palomeras, I., Carbonell, R., Simancas, F., Ayarza, P., Matas, J., González-Lodeiro, F., and Pérez-Estaún, A., 2009, Seismic imaging and modelling of the lithosphere of SW-Iberia: Tectonophysics, v. 472, no. 1–4, p. 148–157.

Fullea, J., Fernandez, M., Afonso, J.C., Verges, J., and Zeyen, H., 2010, The structure and evolution of the lithosphere–asthenosphere boundary beneath the Atlantic–Mediterranean transition region: Lithos, doi: 10.1016/j.lithos.2010.03.003 (in press).

Fuller, B.D., 1967, Two-Dimensional Frequency Analysis and Design of Grid Operators. Mining Geophysics, Volume II (Theory): Tulsa, Oklahoma, Society of Exploration Geophysicists, p. 658–708.

Gallart, J., Vidal, N., Dañobeitia, J.J., and ESCI-Valencia Trough Working Group, 1994, Lateral variations in the deep structure at the Iberian margin of the Valencia trough imaged from seismic reflection methods: Tectonophysics, v. 232, p. 59–75, doi: 10.1016/0040-1951(94)90076-0.

Gallart, J., Salas, R., Guimerá, J., Mas, R., Diaz, J., and Ruiz, M., 2004, A refraction/wide-angle reflection seismic profile through the Iberian Chain: Preliminary report: Geo-Temas, v. 6, no. 2, p. 183–186.

García-Dueñas, V., Banda, E., Torné, M., Córdoba, D., and ESCI-Béticas Working Group, 1994, A deep seismic reflection survey across Betic Chain (southern Spain): First results: Tectonophysics, v. 232, p. 77–89, doi: 10.1016/0040-1951(94)90077-9.

Gómez Ortiz, D., 2001, La Estructura de la Corteza en la Zona Central de la Peninsula Iberica [Ph.D. thesis]: Madrid, Universidad Complutense, 352 p.

Gómez-Ortiz, D., Tejero-López, R., Babín-Vich, R., and Rivas-Ponce, A., 2005, Crustal density structure in the Spanish Central System derived from gravity data analysis (central Spain): Tectonophysics, v. 403, p. 131–149, doi: 10.1016/j.tecto.2005.04.006.

González, A., Torné, M., Córdoba, D., Vidal, N., Matias, L.M., and Díaz, J., 1996, Crustal thinning in the southwestern Iberia margin: Geophysical Research Letters, v. 23, no. 18, p. 2477–2480, doi: 10.1029/96GL02299.

González, A., Córdoba, D., Vegas, R., and Matias, L.M., 1998, Seismic crustal structure in the southwest of the Iberian Peninsula and the Gulf of Cadiz: Tectonophysics, v. 296, p. 317–331, doi: 10.1016/S0040-1951(98)00151-6.

Grad, M., Tiira, T., and ESC Working Group, 2009, The Moho depth map of the European plate: Geophysical Journal International, v. 176, no. 1, p. 279–292, doi: 10.1111/j.1365-246X.2008.03919.x.

Grant, F.S., and West, G.F., 1965, Interpretation Theory in Applied Geophysics: New York, McGraw Hill Book Company, 584 p.

Hatzfeld, D., and Ben Sari, D., 1977, Grands profils sismiques dans la région de l□Arœde Gibraltar: Bulletin de la Société Géologique de France, v. 7, p. 749–756.

ILIHA DSS (Iberian Lithosphere Heterogeneity and Anisotropy Deep Seismic Sounding) Group, 1993, A deep

seismic sounding investigation of lithospheric heterogeneity and anisotropy beneath the Iberian Peninsula: Tectonophysics, v. 221, no. 1, p. 35–51, doi: 10.1016/0040-1951(93)90026-G.

IOC (Intergovernmental Oceanographic Commission), IHO (International Hydrographic Organization), and BODC (British Oceanographic Data Centre), 2003, "Centenary Edition of the GEBCO Digital Atlas": Published on behalf of the Intergovernmental Oceanographic Commission and the International Hydrographic Organization as part of the General Bathymetric Chart of the Oceans; Liverpool, British Oceanographic Data Centre, CD-ROM.

Julià, J., and Mejía, J., 2004, Thickness and Vp/Vs ratio variation in the Iberian crust: Geophysical Journal International, v. 156, p. 59–72, doi: 10.1111/j.1365-246X.2004.02127.x.

Kanamori, H., 1963, A new method for downward continuation of two-dimensional gravity distribution: Proceedings of the Japan Academy, v. 39, p. 469.

Lefort, J.P., and Agarwal, B.N.P., 1996, Gravity evidence for an Alpine buckling of the crust beneath the Paris Basin: Tectonophysics, v. 258, p. 1–14, doi: 10.1016/0040-1951(95)00148-4.

Lefort, J.P., and Agarwal, B.N.P., 1999, Of what is the center of the Ibero-Armorican Arc composed?: Tectonophysics, v. 302, p. 71–81, doi: 10.1016/S0040-1951(98)00275-3.

Lefort, J.P., and Agarwal, B.N.P., 2000, Gravity and geomorphologic evidences for a large crustal bulge cutting across Brittany (France): A tectonic response to the actual closure of Biscay Bay: Tectonophysics, v. 323, p. 149–162, doi: 10.1016/S0040-1951(00)00103-7.

Lefort, J.P., and Agarwal, B.N.P., 2002, Topography of the Moho undulations in France from gravity data: Their age and origin: Tectonophysics, v. 350, p. 193–213, doi: 10.1016/S0040-1951(02)00114-2.

Lefort, J.P., Agarwal, B.N.P., and Jaffal, M., 1998, A tentative chronology of the Moho undulations in the Celtic sea region: Journal of Geodynamics, v. 27, p. 161–174, doi: 10.1016/S0264-3707(98)00005-2.

Martin, M.A., 1962, Frequency Domain Applications in Data Processing: Technical Information Series 57SD340, Technical Data Centre, Nose Cone section, MOSD (Missile and Ordnance Systems Department), Philadelphia, 32 p.

Matias, L.M., 1996, A Sismologia Experimental na Modelação da Estrutura da Crusta em Portugal Continental [Ph.D. thesis]: Lisbon, Portugal, Universidad Lisboa, 398 p.

Matte, Ph., 1991, Accretionary history and crustal evolution of the Variscan belt in Western Europe: Tectonophysics, v. 196, p. 309–337, doi: 10.1016/0040-1951(91)90328-P.

McCllelan, J.H., 1973, The design of two-dimensional digital filter by transformation, *in* Proceedings of the 7th Annual Princeton Conference on Information Sciences and Systems, Princeton, New Jersey, p. 247–251.

Mezcua, J., Gil, A., and Benarroch, R., 1996, Estudio Gravimétrico de la Península Ibérica y Baleares: Madrid, Instituto Geográfico Nacional, 7 p.

Muñoz, J.A., 1992, Evolution of a continental collision belt. ECORS Pyrenees crustal balanced cross-section, *in* McClay, K.R., ed., Thrust Tectonics: London, Chapman and Hall, p. 235–246.

Nabighian, M.N., Grauch, V.J.S., Hansen, R.O., LaFehr, T.R., Li, Y., Pearson, W.C., Pierce, J.W., Phillips, J.D., and Ruder, M.E., 2005, Historical development of the gravity method in exploration: Geophysics, v. 70, p. 63–89, doi. 10.1190/1.2133785.

Palomeras, I., Carbonell, R., Flecha, I., Simancas, F., Ayarza, P., Matas, J., Martinez-Poyatos, D., Azor, A., González-Lodeiro, F., and Pérez-Estaún, A., 2008, The nature of the lithosphere across the Variscan orogen of SW Iberia: Dense wide-angle seismic refraction data: Journal of Geophysical Research, v. 114, B02302, doi: 10.1029/2007JB005050.

Panza, F.G., Raykova, R.B., Carminati, E., and Doglioni, C., 2007, Upper mantle flow in the western Mediterranean: Earth and Planetary Science Letters, v. 257, p. 200–214, doi: 10.1016/j.epsl.2007.02.032.

Pedreira, D., Pulgar, J.A., Gallart, J., and Díaz, J., 2003, Seismic evidence of Alpine crustal thickening and wedging from the western Pyrenees to the Cantabrian Mountains (north Iberia): Journal of Geophysical Research, v. 108, no. B4, p. ETG 10-1–ETG 10-21, doi: 10.1029/2001JB001667.

Piromallo, C., and Morelli, A., 2003, P wave tomography of the mantle under the Alpine-Mediterranean area: Journal of Geophysical Research, v. 108, no. B2, p. 2065, doi: 10.1029/2002JB001757.

Pulgar, J.S., Gallart, J., Fernández-Viejo, G., Pérez-Estaún, A., Álvarez-Marrón, J., and ESCIN Group, 1996, Seismic image of the Cantabrian Mountains in the western extension of the Pyrenees from integrated ESCIN reflection and refraction data: Tectonophysics, v. 264, p. 1–19, doi: 10.1016/S0040-1951(96)00114-X.

Ribeiro, A., 2006, A evoluçao geodinâmica de Portugal, *in* Dias, R., Araujo, A., Terrinaha, P., and Kullberg, M., eds., Geologia de Portugal na Contexto da Iberia: Evora, University of Evora, p. 1–27.

Rivero, L., Pinto, V., and Casas, A., 2002, Moho depth structure of the eastern part of the Pyrenean belt derived from gravity data: Journal of Geodynamics, v. 33, p. 315–332, doi: 10.1016/S0264-3707(01)00073-4.

Roy, A., 1962, Ambiguity in geophysical interpretation: Geophysics, v. 27, p. 90–99, doi: 10.1190/1.1438985.

Salas, R., and Casas, A., 1993, Mesozoic extensional tectonics, stratigraphy and crustal evolution during the Alpine cycle of the eastern Iberian basin: Tectonophysics, v. 228, p. 33–55, doi: 10.1016/0040-1951(93)90213-4.

Sánchez Jiménez, N., 2003, Estructura Gravimétrica y Magnética de la Corteza del Suroeste Peninsular (Zona Subportuguesa y Zona de Ossa-Morena), Spain [Ph.D. thesis]: Madrid, Spain, Universidad Complutense, 243 p.

Simancas, J.F., Carbonell, R., González Lodeiro, F., Pérez Estaún, A., Juhlin, C., Ayarza, P., Kashubin, A., Azor, A., Martínez Poyatos, D., Almodóvar, G.R., Pascual, E., Sáez, R., and Expósito, I., 2003, The crustal structure of the transpressional Variscan orogen of the SW Iberia: The IBERSEIS Deep Seismic Reflection Profile: Tectonics, v. 22, no. 6, p. 1–16.

Skeels, D.C., 1967, What is residual gravity?: Geophysics, v. 32, p. 872–876, doi: 10.1190/1.1439896.

Spector, A., and Grant, F.S., 1970, Statistical methods for interpreting aeromagnetic data: Geophysics, v. 35, p. 293–302, doi: 10.1190/1.1440092.

Suriñach, E., and Chavez, R.E., 1996, A 3D gravimetric crustal model for the northeastern region of the Iberian Peninsula: Geophysical Research Letters, v. 23, p. 2457–2460, doi: 10.1029/96GL02203.

Suriñach, E., and Vegas, R., 1988, Lateral inhomogeneities of the Hercynian crust in central Spain: Physics of the Earth and Planetary Interiors, v. 51, p. 226–234, doi: 10.1016/0031-9201(88)90049-0.

Syberg, F.J.R., 1972, A Fourier method for the regional-residual problem of potential fields: Geophysical Prospecting, v. 20, p. 47–75, doi: 10.1111/j.1365-2478.1972.tb00619.x.

Takeuchi, H., and Saito, M., 1964, Numerical tables useful in three-dimensional gravity interpretation: Bulletin of the Earthquake Research Institute, v. 42, p. 39.

Tejero, R., Carbonell, R., Ayarza, P., Azor, A., Garcia-Lobón, J.L., González Cuadra, P., González Lodeiro, F., Jabaloy, A., Mansilla, L., Martín-Parra, L.M., Martínez Poyatos, D., Matas, J., Palomeras, I., Pérez-Estaún, A., and Simancas, J.F., 2008, The ALCUDIA Seismic Profile: An image of the Central Iberian zone (Southern Iberian Variscides, Spain): Geo-Temas, v. 10, p. 285.

Téllez, J., Matias, L.M., Córdoba, D., and Mendes-Victor, L.A., 1993, Structure of the crust in the schistose domain of Galicia-Tras-os-Montes (NW Iberian Peninsula), *in* Badal, J., Gallart, J., and Paulssen, H., eds., Seismic Studies of the Iberian Peninsula: Tectonophysics, v. 221, p. 81–93.

Torné, M., and Banda, E., 1992, Crustal thinning from the Betic Cordillera to the Alboran Sea: Geo-Marine Letters, v. 12, p. 76–81, doi: 10.1007/BF02084915.

Tsuboi, C., 1979, Gravity: London, Allen and Unwin, 254 p.

Tsuboi, C., Oldham, C.H.G., and Waithman, V.B., 1958, Numerical tables facilitating three-dimensional gravity interpretations: Journal of Physics of the Earth, v. 6, p. 7.

Working Group for Deep Seismic Sounding in Alboran 1974, 1978, Crustal seismic profiles in the Alboran sea—Preliminary results: Pageoph, v. 116, p. 166–180.

Zeyen, H.J., Banda, E., Gallart, J., and Ansorge, J., 1985, A wide angle seismic reconnaissance survey of the crust and upper mantle in the Celtiberian Chain of eastern Spain: Earth and Planetary Science Letters, v. 75, p. 393–402, doi: 10.1016/0012-821X(85)90182-7.

Zurflueh, E.G., 1967, Application of two dimensional linear wavelength filtering: Geophysics, v. 32, p. 1015–1035, doi: 10.1190/1.1439905.

Manuscript Received 15 December 2009
Revised Manuscript Received 29 July 2010
Manuscript Accepted 3 August 2010

Printed in the USA